



Magnetoresistance Hysteresis Evolution in the Granular Y–Ba–Cu–O High-Temperature Superconductor in a Wide Temperature Range

S. V. Semenov¹ · D. A. Balaev¹

Received: 17 January 2019 / Accepted: 29 January 2019 / Published online: 13 February 2019
© Springer Science+Business Media, LLC, part of Springer Nature 2019

Abstract

The temperature evolution of the magnetoresistance hysteresis in the granular $\text{YBa}_2\text{Cu}_3\text{O}_{7-\delta}$ high-temperature ($T_C \approx 92$ K) superconductor has been investigated. The measurements have been performed in the high-temperature region (78–90 K) and at the liquid helium temperature (4.2 K). The results obtained have been analyzed using the developed model of the behavior of transport properties of a granular high-temperature superconductor in an external magnetic field. Within the discussed model, the dissipation of the grain boundary subsystem is determined by the intergrain spacing-averaged effective field B_{eff} , which is a superposition of external field H and the field induced by the magnetic moments of superconducting grains. Such a consideration yields the expression $B_{\text{eff}}(H) = H - 4\pi M(H) \alpha$ for the effective field in the intergrain medium, where $M(H)$ is the experimental hysteretic dependence of magnetization and α is the parameter of magnetic flux crowding in the intergrain medium. Here, the magnetoresistance is assumed to be proportional to the absolute value of the effective field: $R(H) \sim |B_{\text{eff}}(H)|$. Analysis of the experimental $R(H)$ and $M(H)$ dependences obtained under the same conditions for the investigated high-temperature superconductor sample showed that in the high-temperature region this parameter is $\alpha \approx 25$. At the low temperature (4.2 K), we may state that the degree of flux crowding increases and the estimated α value is ~ 50 . The estimates made are indicative of the strong effect of flux compression in the intergrain medium on the magnetotransport properties of the investigated granular high-temperature superconductor system. Possible reasons for a discrepancy between the developed model concepts and experimentally observed low-temperature $R(H)$ hysteresis are analyzed.

Keywords Granular HTSC · YBCO · Magnetoresistance hysteresis · Effective field · Intergrain medium · Magnetic flux compression

1 Introduction

The magnetic and magnetotransport properties of granular high-temperature superconductors (HTSs) suggest that it would be reasonable to consider these materials to consist of two superconducting subsystems. The first (main) subsystem is formed from HTS grains. The second subsystem comprises grain boundaries. The relative volume fraction of the second subsystem is incomparably smaller than the volume fraction of superconducting grains, since the geometrical length of a

boundary is about 1 nm [1–5], while the grain size ranges from fractions of a micron to tens of microns. However, due to the small HTS coherence length (about 1 nm as well), the superconductivity in the grain boundary region is essentially weakened and the superconducting current transport through the boundaries is implemented via the Josephson effect. Therefore, the transport properties of granular HTSs are mainly determined by the dissipation processes in the grain boundary subsystem. Consequently, a granular HTS can be considered as a two-phase system with the strictly segregated dissipation processes; specifically, the density j_{CGB} of the critical current through the grain boundary is much lower than the intragrain critical current density j_{CG} [6–8]:

$$j_{\text{CGB}} \ll j_{\text{CG}}. \quad (1)$$

The abovementioned subsystems, however, interact with each other. Their coupling is especially pronounced in an

✉ S. V. Semenov
svsemenov@iph.krasn.ru

¹ Kirensky Institute of Physics, Federal Research Center KSC SB RAS, Krasnoyarsk, Russia 660036

applied magnetic field, i.e., when studying the magnetotransport properties of a granular HTS, e.g., its magnetoresistance¹ $R(H)$ [8–19]. The magnetic moments of HTS grains affect the intergrain spacing; as a result, instead of external field H induced by a solenoid, the grain boundaries appear in the effective field B_{eff} , which is a superposition of the external field H and field B_{ind} induced by the magnetic moments of HTS grains:

$$B_{\text{eff}} = H + B_{\text{ind}}. \quad (2)$$

Taking into account the well-known magnetization hysteresis of superconductors, the field B_{ind} and, consequently, the effective field B_{eff} in the grain boundary region will also be hysteretic functions of the external field. Since the dissipation in superconductors is related to the magnetic field value (here, the effective field value, $R \sim B_{\text{eff}}$), the magnetotransport properties of granular HTSs exhibit the hysteretic phenomena.

These concepts were used to qualitatively describe the intriguing features of the magnetotransport properties of granular HTSs, including the magnetic field hysteresis of the critical current $J_C(H)$ [20–25] and magnetoresistance $R(H)$ [13–19, 23–25] and the temperature hysteresis of electrical resistance $R(T)$ at $H = \text{const}$ [16, 26]. Consideration of the grain boundary subsystem in a certain effective field [13] made it possible to explain the well-known magnetoresistance anisotropy in granular HTSs with respect to the mutual orientation of the external field and transport current direction [13, 27–29].

The described model of the behavior of a granular HTS in an external field has been essentially developed after making an obvious assumption about the direct relation of the induced field B_{ind} to the experimental field dependence of magnetization $M(H)$: $B_{\text{ind}}(H) \sim |M(H)|$ [15, 30]. In other words, the effective field in the intergrain medium is determined, to a great extent, by the behavior of magnetization. Indeed, the thorough comparison of the $R(H)$ and $M(H)$ hysteretic dependences made it possible to adequately explain the existence of a local $R(H)$ maximum [15] and establish the origin of specific features of the relaxation behavior of the resistance in a dc magnetic field [19, 30–32].

In addition, as was mentioned first in [13], the magnetic flux crowding can occur in the grain boundary region. This phenomenon can take place when the geometrical length of a grain boundary is much smaller than the grain size, which is the case in granular HTS materials. In fact, the effective field in the intergrain medium can be much stronger than the external field and the field induced by superconducting grains [19, 30, 33, 34]. This crowding is taken into account in the expression for the effective field in the intergrain medium [19, 30].

$$B_{\text{eff}}(H) = |H - 4\pi M(H)| \alpha \quad (3)$$

¹ Hereinafter, the drop of voltage U divided by transport current I , i.e., $R = U/I$, is referred to as resistance.

In Eq. (2), $M(H)$ is the experimental magnetic hysteresis loop and α is the parameter of crowding of the magnetic flux lines from superconducting grains in the intergrain medium; at $\alpha \gg 1$, the crowding is significant. It was found that the parameter α of the HTS systems is much higher than unity, and many experimental features of the $R(H)$ dependences are explained under the assumption of $\alpha \sim 10$ – 20 [19, 30, 34].

The reported results were obtained at the nitrogen temperature. As was shown in study [35], the parameter α of magnetic flux crowding in the yttrium HTS system is almost temperature-independent in the range of 77–90 K (at a critical temperature of $T_C = 92$ K). In our opinion, these investigations can be extended to the low-temperature region. To further develop the model of the behavior of a granular HTS in an external field, here we analyze the magnetoresistance hysteresis in the granular $\text{YBa}_2\text{Cu}_3\text{O}_{7-\delta}$ HTS at the liquid helium temperature and compare the obtained data with the results for the high-temperature region.

2 Experimental

The $\text{YBa}_2\text{Cu}_3\text{O}_{7-\delta}$ HTS sample was synthesized by a standard solid-state synthesis technique from initial oxides with three intermediate grindings. The X-ray structural analysis showed that all reflections correspond to the 1–2–3 HTSs without inclusions of foreign phases.

Scanning electron microscopy and energy-dispersive spectrometry investigations were carried out on a Hitachi-TM 3000 electron microscope. Figure 1 presents typical data on the sample microstructure. One can see a granular structure with an average grain size of about 5 μm . According to the energy-dispersive spectrometry analysis data, the element ratio corresponds to the chemical formula $\text{YBa}_2\text{Cu}_3\text{O}_{7-\delta}$. The physical density of the investigated sample was $\sim 88\%$ of the theoretical $\text{YBa}_2\text{Cu}_3\text{O}_{7-\delta}$ density.

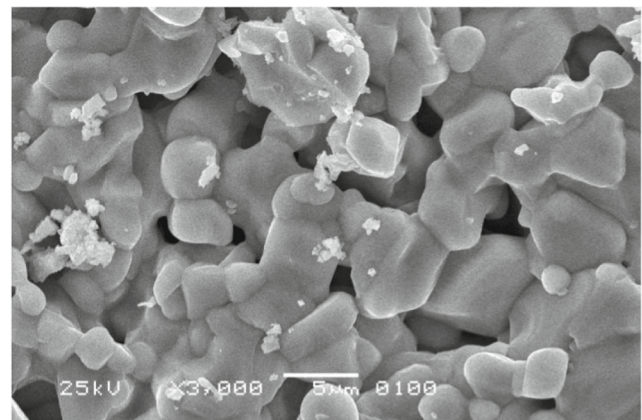


Fig. 1 Scanning electron microscopy image of the typical microstructure of the $\text{YBa}_2\text{Cu}_3\text{O}_{7-\delta}$ sample

It is well known that the final annealing conditions affect the critical current density j_C in granular HTSs [3, 5]. In our case, the parameter j_C was not purposefully increased and the final annealing at 915°C for 20 h was performed. The j_C values in zero external field for the sample under study were $\sim 15 \text{ A/cm}^2$ at $T = 77 \text{ K}$ and $\sim 170 \text{ A/cm}^2$ at $T = 4.2 \text{ K}$.

The magnetotransport measurements were performed by a standard four-probe technique under the zero-field cooling conditions. Specimens about $0.4 \times 0.4 \times 7 \text{ mm}^3$ in size for the magnetotransport investigations were cut and the transport current I flowed along to their longer sides. The external field was applied perpendicular to the direction of the macroscopic transport current j .

Gold-plated pressed electric contacts were used. During the $R(H)$ measurements in the temperature range of 77–90 K, the specimen was in the helium heat-exchange atmosphere; the external field was induced by an electromagnet; the transport current was $I = 3 \text{ mA}$. The $R(H)$ dependence at a temperature of 4.2 K was measured by placing the specimen directly in a cryostat filled with liquid helium; an external field of up to $\pm 60 \text{ kOe}$ was induced by a superconducting solenoid. To observe a non-zero magnetoresistance in low temperatures, it is necessary to use much higher transport currents than in the region of the liquid nitrogen temperature. The data analyzed in Sect. 3.4 were obtained at $I = 175 \text{ mA}$ ($T = 4.2 \text{ K}$). Under these conditions, the Joule heat release on side contacts did not lead to sample heating. The magnetoresistance data in the high-temperature region and at 4.2 K were obtained using the same specimen.

The magnetic properties were studied on a vibrating sample magnetometer under the external conditions, including the external magnetic field sweep rate, corresponding to the magnetotransport measurements.

According to the transport measurement data (Fig. 2a), the temperature corresponding to the onset of the transition to the superconducting state was $\sim 92 \text{ K}$. This is consistent with the magnetic measurement data presented in Fig. 2b. Thus, the investigated $\text{YBa}_2\text{Cu}_3\text{O}_{7-\delta}$ sample exhibits the properties typical of the granular yttrium HTS materials, which gives us grounds to generalize our conclusions to, at least, the class of granular materials of the HTS system under study.

3 Results and Discussion

3.1 Experimental Justification of Existence of Two Superconducting Subsystems (Grain Boundaries and HTS Grains)

The $R(T)$ dependences presented in Fig. 2a were obtained in different external fields. A fairly sharp resistance jump weakly dependent on the external field unambiguously corresponds to the superconducting transition in the HTS grain subsystem, and the smooth $R(T)$ portion reflects the transition of the grain

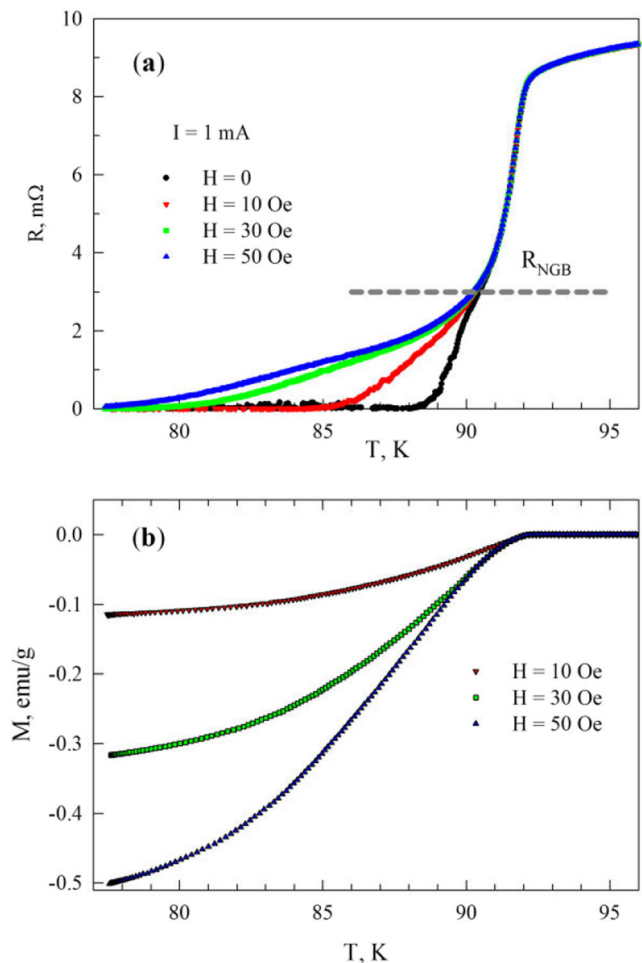


Fig. 2 Temperature dependences of **a** resistance $R(T)$ and **b** magnetization $M(T)$ in different external fields. On **a**, the value of R_{NGB} (the resistance of the grain boundary subsystem) is shown

boundary subsystem to the superconducting state [6, 13, 19, 25–27, 36–41]. It is worth noting that the magnetic contribution of the grain boundary subsystem under the conditions corresponding to the experiments illustrated in Fig. 2a is very small [7, 42]: the $M(T)$ dependences shown in Fig. 2b contain no anomalies related to the transition in the grain boundary subsystem. Such a behavior is characteristic of granular HTSs and obeys Eq. (1). Using the data shown in Fig. 2a, one can obtain the total resistance R_{NGB} of the grain boundary subsystem. In the granular HTSs of the classical yttrium, bismuth, and lanthanum systems, the hysteresis of magnetotransport properties is observed in the region of resistances lower than R_{NGB} [8–19, 23–25, 30–35, 43, 44].

Figure 3 shows the $M(H)$ hysteretic dependences for the investigated sample at temperatures of 80 and 4.2 K. According to the Bean formula, the intragrain current density j_{CG} can be estimated as $j_{\text{CG}} (\text{A/cm}^2) \sim 30 \Delta M (\text{emu/cm}^3)/d (\text{cm})$, where ΔM is the magnetic hysteresis loop height [45]. Substituting the average grain size ($d \sim 5 \mu\text{m}$) and magnetization (Fig. 4) in an external field of $H \approx 100 \text{ Oe}$ yields j_{CG} values of about 1.5×10^5 and

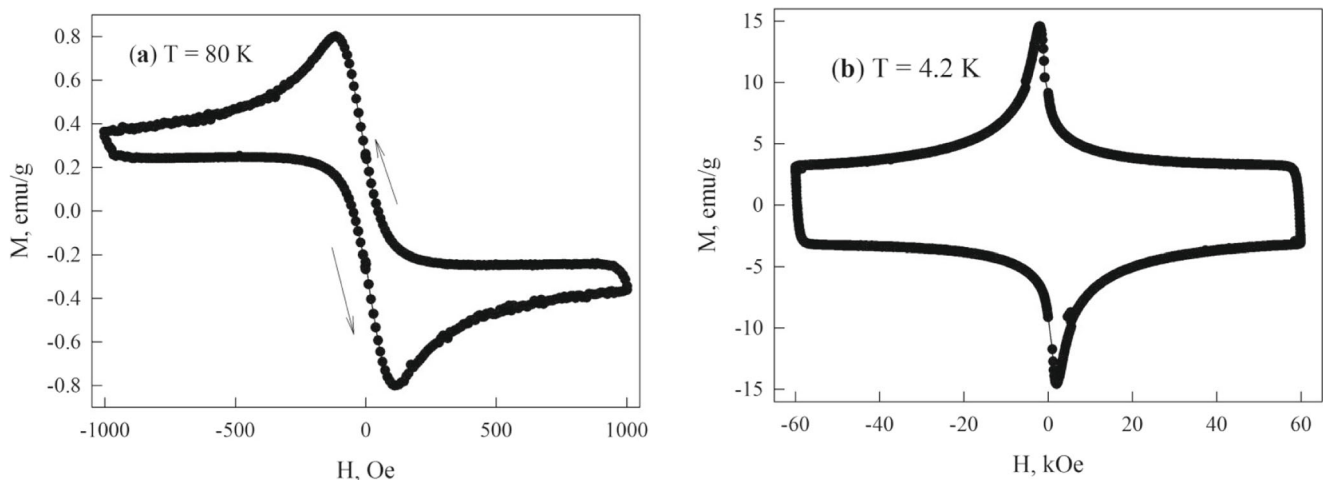


Fig. 3 Magnetization hysteresis $M(H)$ of the investigated sample at **a** $T = 80$ and **b** 4.2 K. Arrows show the direction of variation in the external field H

2.3×10^6 A/cm² at temperatures of 80 and 4.2 K, respectively. Comparing the obtained values with the critical current densities (see Sect. 2), we may be certain that Eq. (1) is valid.

The shape evolution of the $M(H)$ dependences and j_{CG} growth with decreasing temperature are typical of granular HTS samples [46–48]. The experimental conditions, including temperature and external field, in Fig. 3 are analogous to the conditions for obtaining the $R(H)$ dependences discussed below (Sects. 3.3 and 3.4) on the basis of the obtained data.

3.2 Model

Figure 4 shows a schematic of idealized magnetic flux lines in the intergrain medium of a granular HTS. Ovals show the HTS grains. The direction of macroscopic transport current j is perpendicular to the external field H ; in this representation, the microscopic current I_m is co-directed with j . It is assumed that there is no dissipation within the HTS grains (Eq. (1)). The magnetic moments M_{G1} and M_{G2} of HTS grains are antiparallel to the external field when the latter increases ($H = H_{inc}$). It can be seen in Fig. 4a that the magnetic flux lines from M_G pass through the intergrain medium (spacing between grains) and are closed to the top of grains. When the external field decreases ($H = H_{dec}$), the magnetic moments of superconducting grains, according to the generally accepted concepts, are co-directed with the external field (see also Fig. 3) and the direction of the magnetic flux lines from $M_{G1,2}$ will be opposite to that shown in Fig. 4. Thus, the magnetic moments of HTS grains induce the field B_{ind} in the intergrain medium. This field has different directions at $H = H_{inc}$ and $H = H_{dec}$. It is reasonable to relate the B_{ind} value to the sample magnetization $M(H)$ and, taking into account the directions of vectors H , $M_{G1,2}$, and B_{ind} (Fig. 4), we obtain

$$B_{ind}(H) \sim -4\pi M(H)\alpha, \quad (4)$$

where the parameter α includes the averaged effect of grain demagnetizing factors and crowding of the magnetic flux lines.

In real granular systems, the intergrain spacings are much smaller than the grain size, which can lead to the flux crowding schematically illustrated in Fig. 4b. It is obvious that if the parameter α in Eq. (4) is much higher than unity (the effect of demagnetizing factors of the grain shape is maximum) than this fact proves the magnetic flux crowding in the intergrain spacing [19, 30, 34, 35]. The magnetoresistance R is a function of the effective field B_{eff} and, since the dissipation processes are independent of the magnetic field sign, we obtain, with regard to Eqs. (2) and (4), the expression for the effective field in the form of Eq. (3): $B_{eff}(H) = |H - 4\pi M(H)\alpha|$.

The technique for determining the parameter α proposed in [19, 30, 34, 35, 49] includes the comparison of $R(H)$ hysteretic dependences (experimental) and $B_{eff}(H)$ (using the experimental $M(H)$ data) at different α values. In this case, the field widths of the $R(H)$ and $B_{eff}(H)$ hysteretic dependences, rather than the R and B_{eff} values, are compared. This is based on the independence of the field width of the $R(H)$ hysteresis established earlier for different granular HTS systems at different transport currents in [25, 32, 33, 35, 50, 51]. The field width of the hysteresis is determined as a segment between the descending and ascending branches of the hysteretic dependences at $R(H_{inc}) = R(H_{dec})$ for the $R(H)$ dependence and $B_{eff}(H_{inc}) = B_{eff}(H_{dec})$ for the $B_{eff}(H)$ dependence [30, 34, 35, 49]. In fact, such a comparison of the experimental data does not concern the R and B_{eff} values, but only operates with the field width of the hysteresis. The technique used allowed us to establish that the α value of the granular yttrium HTS is about 20–25 at $H \perp j$ [34, 35, 49], which is the manifestation of the considerable flux compression in the intergrain medium. In addition, as was shown in [35], the α value is almost temperature-independent in the range of 77–90 K. Note that in the procedure used in the above-cited works, the parameter α was assumed to be independent of external field, although there was a certain discrepancy between the $R(H)$ and $B_{eff}(H)$ hysteresis at $H = H_{dec}$ in weak fields [19, 30, 34, 35].

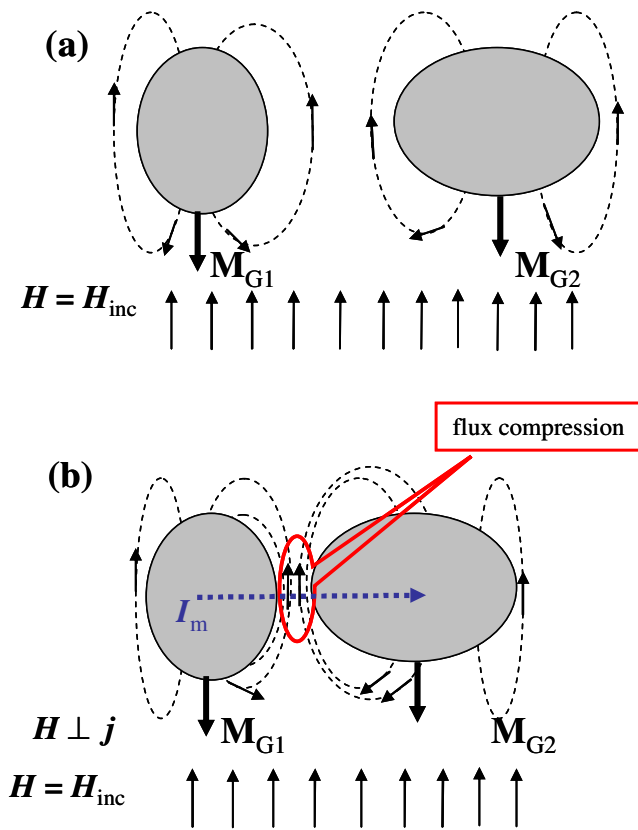


Fig. 4 Schematic of the magnetic induction lines in the intergrain medium of a granular HTS. Upward arrows show the direction of external field H and dashed lines show the magnetic flux lines induced by the magnetic moments $M_{G1,2}$ (bold arrows) of HTS grains (ovals). Arrows in the magnetic flux lines show their direction for the case of increasing external field ($H = H_{inc}$). Different distances between grains in **a** and **b** schematically illustrate the magnetic flux compression in the intergrain spacings for close grains. The dotted line in **b** shows the direction of microscopic current I_m

3.3 Magnetic Flux Compression in the High-Temperature Region

Figure 5a shows the $R(H)$ dependence at $T = 80$ K (the transport current is $I = 3$ mA). Let us analyze the hysteretic behavior of this dependence using the abovementioned approach. The horizontal lines in Fig. 5a show examples of determining the field width of the magnetoresistance hysteresis $\Delta H = H_{dec} - H_{inc}$ under the condition $R(H_{dec}) = R(H_{inc})$ at $H_{dec} = 950$ and 500 Oe. The experimental $R(H)$ data agree well with the parameter ΔH of the calculated $B_{eff}(H)$ dependence at $\alpha \approx 25$. Figure 5b presents the $B_{eff}(H)$ dependence obtained at $\alpha \approx 25$ on the basis of the $M(H)$ data shown in Fig. 3a. Comparison of the field widths ΔH of the hysteresis in Fig. 5a, b shows that the ΔH values at $H_{dec} = 950$ and 500 Oe are similar.

Figure 6 presents the $\Delta H(H_{dec})$ dependences obtained from the experimental $R(H)$ hysteretic dependence and $B_{eff}(H)$ dependences at different α values. For the sake of simplicity, when calculating the $\Delta H(H_{dec})$ values (see Fig. 6 and below in Sect. 3.3), we did not take into account the $\Delta H(H_{dec})$

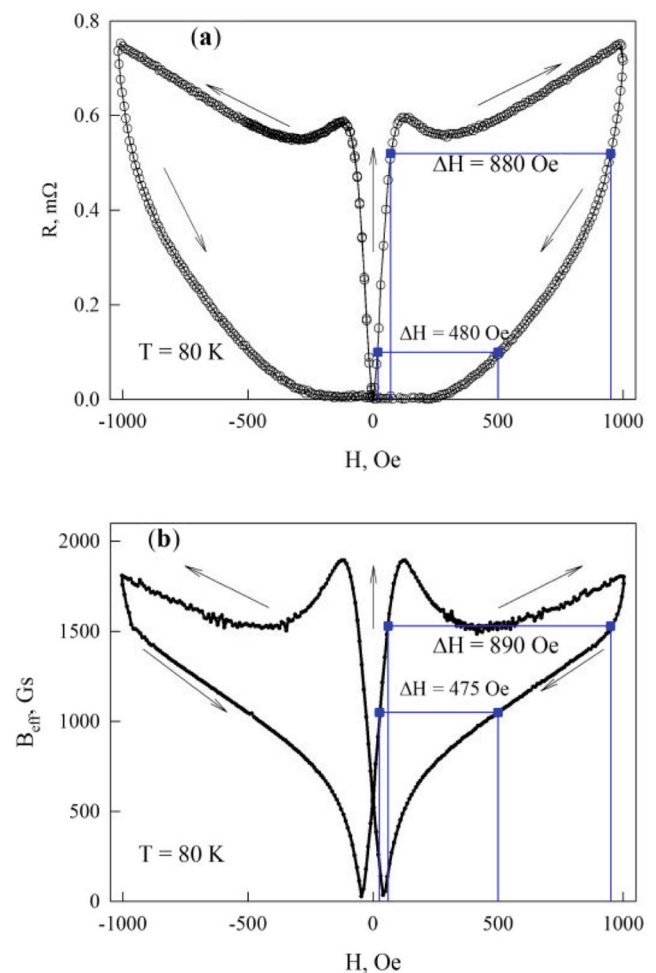


Fig. 5 Hysteric dependences of **a** magnetoresistance $R(H)$ and **b** effective field $B_{eff}(H)$ for the sample under study at $T = 80$ K. The $B_{eff}(H)$ dependence is built using Eq. (3) from the $M(H)$ data (Fig. 3a) at $\alpha = 25$. Horizontal lines between symbols show determination of the field width ΔH of the hysteresis at $H_{dec} = 950$ and 500 Oe. Arrows show the external field variation direction

dependence two valuedness caused by the presence of a local maximum in the $R(H_{inc})$ dependences (at high temperatures) and $B_{eff}(H_{inc})$ dependences. As a result, a sharp jump is observed in the range from H_{max} to field H , which corresponds to the non-monotonic behavior of the $R(H_{inc})$ or $B_{eff}(H_{inc})$ dependences, instead of the two-valued function $\Delta H(H_{dec})$. It can be seen in Fig. 6 that the best agreement between the ΔH values for the magnetoresistance and effective field is obtained at $\alpha \approx 25$.

The determined α value (~ 25) is similar to the values obtained by us in [34, 35, 49], although the investigated samples had different characteristics. In particular, in study [35], the critical current density at 77 K in zero external field was 150 A/cm^2 , while the j_c value for the sample examined here is smaller by an order of magnitude (15 A/cm^2). For the sample investigated in this work, we obtained also the α values above the nitrogen temperature (82–88 K) and found $\alpha \approx 25$, which is consistent with the conclusions made in [35]. Thus,

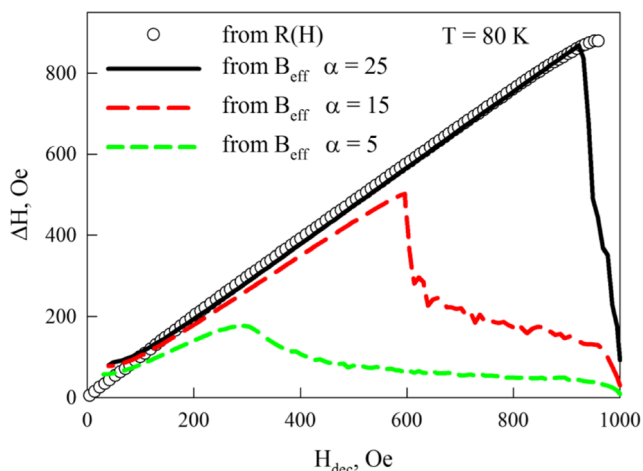


Fig. 6 Field dependence ΔH of the hysteresis for the experimental $R(H)$ dependence at $T = 80$ K for the data from Fig. 5a (symbols) and hysteresis of the effective field $B_{\text{eff}}(H)$ calculated using Eq. (3) from the $M(H)$ data (Fig. 3a) at different α values (lines)

having generalized the results for the different yttrium subsystem samples [19, 30, 34, 35, 49], we may conclude that this class of granular materials is characterized by a fairly strong flux compression and the degree of flux crowding weakly depends on temperature in the high-temperature region.

3.4 Magnetoresistance Hysteresis and Magnetic Flux Compression at 4.2 K

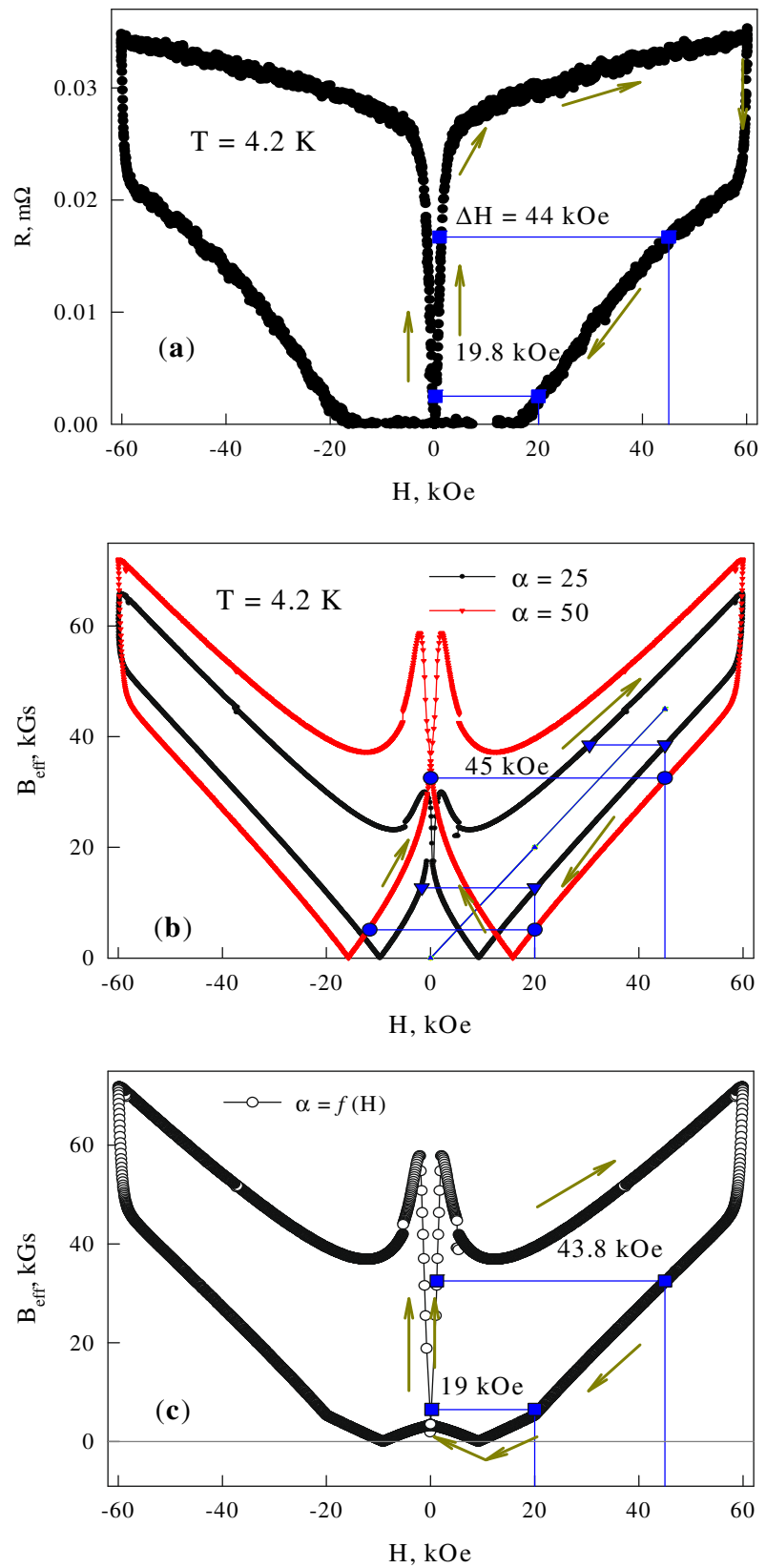
Figure 7a presents the $R(H)$ hysteretic dependence for the investigated sample at $T = 4.2$ K. Let us analyze the hysteretic behavior of the $R(H)$ dependence using the approach described in Sect. 3.2. Figure 7b shows the $B_{\text{eff}}(H)$ dependences calculated using Eq. (3) at $\alpha = 25$ and 50 from the $M(H)$ data in Fig. 3b. We compare the field widths of the hysteresis for the $R(H)$ data from Fig. 7a and $B_{\text{eff}}(H)$ data from Fig. 7b at some characteristic points of the descending branch $H = H_{\text{dec}}$ of the hysteretic dependences. The lengths of horizontal lines in Fig. 7 show the ΔH values ($\Delta H = H_{\text{dec}} - H_{\text{inc}}$) for the magnetoresistance (Fig. 7a) and effective field hysteresis (Fig. 7b, c) at $H_{\text{dec}} = 20$ and 45 kOe. Comparison of the data presented in Fig. 7a, b shows that the value ΔH ($H_{\text{dec}} = 45$ kOe) in the $B_{\text{eff}}(H)$ dependence at $\alpha = 25$ is significantly lower. At the same time, in the strong field region, the $B_{\text{eff}}(H)$ hysteresis width becomes similar to the ΔH value of the $R(H)$ hysteresis if the parameter α will be larger. This is clear from the comparison of the ΔH ($H_{\text{dec}} = 45$ kOe) values of the $B_{\text{eff}}(H)$ dependence at $\alpha = 50$ (Fig. 7b) and $R(H)$ dependence (Fig. 7a). In other words, the sufficiently large field widths of the magnetoresistance hysteresis in the high-field region show that the parameter α , which characterizes the crowding of the magnetic flux lines in the intergrain medium, grows at low temperatures.

This enhancement of the magnetic flux crowding at low temperatures can occur due to the proximity effect [52]. On one hand, the geometrical length of the intergrain boundary, i.e., the spatial region where neighboring grains are agglomerated and the crystal order is broken, remains invariable. At the same time, as the temperature decreases, the superconductor order parameter in the grains forming grain–boundary–grain Josephson junctions increases and, in the classical representation of the proximity effect [52], the overlap of wave functions of the neighboring superconducting grains will be larger at low temperature. In the description of weakly bound superconductors, this is considered as a decrease in the effective length of the intergrain boundary at low temperatures [52, 53]. As a result, the degree of magnetic flux compression can increase (the parameter α will increase). In addition, note that the temperature range, where the parameter α was found to be approximately constant ($\alpha \approx 25$), is rather narrow (77–88 K) and the doubling of the α value at $T = 4.2$ K seems quite acceptable.

Nevertheless, comparing the data presented in Fig. 7a, b, we may conclude that in fields H_{dec} weaker than 30–40 kOe, the $B_{\text{eff}}(H)$ dependences, both at $\alpha \approx 25$ and $\alpha \approx 50$, poorly describe the magnetoresistance hysteresis behavior. This is shown by the comparison of the horizontal segment lengths in Fig. 7a, b at $H_{\text{dec}} = 20$ kOe. For the $R(H)$ data, the H_{inc} values are positive at $H_{\text{dec}} = 20$ kOe (Fig. 7a), while for the $B_{\text{eff}}(H)$ dependences, the H_{inc} values corresponding to $B_{\text{eff}}(H_{\text{dec}} = 20 \text{ kOe}) = B_{\text{eff}}(H_{\text{inc}})$ are negative (Fig. 7b). As we demonstrated previously, in the region of low H_{dec} values at high temperatures, the consistency between the $B_{\text{eff}}(H)$ and $R(H)$ behaviors is not very good [19, 30, 34, 35, 49]. In this field range, the $R(H_{\text{dec}})$ dependences have minima [14–18, 23, 25, 32–34, 50]. When the external field decreases ($H = H_{\text{dec}}$), the sample magnetization takes positive values (Fig. 3) and the \mathbf{M}_G directions coincide with the external field direction (Fig. 3). In this case, the field induced by \mathbf{M}_G in the intergrain medium will compensate the external field H and the minimum resistance (effective field) corresponds to the maximum compensation of these two contributions to B_{eff} .

The minimum in the $R(H_{\text{dec}})$ dependence is observed at the fairly high transport current; at the low currents, the zero resistance is experimentally observed in a certain H_{dec} range [14–18, 23, 25, 32–34, 50], which is seen in Figs. 7a and 5a. As was mentioned in [19, 34, 35, 49], the agreement between the $R(H_{\text{dec}})$ and $B_{\text{eff}}(H_{\text{dec}})$ minima positions can be obtained assuming the parameter α to decrease in the relatively weak H_{dec} fields. The H_{dec} range where Eq. (3) for the effective field at $\alpha = \text{const}$ already poorly reproduced the $R(H)$ hysteretic feature was fairly narrow (narrower than 100 Oe) [19, 34, 35, 49]. In our previous studies and in the present work, in the $B_{\text{eff}}(H)$ calculations using Eq. (3), the parameter α was assumed to be field-independent ($\alpha = \text{const}$). Concerning the data obtained at $T = 4.2$ K, we may state that this assumption is not quite adequate in a certain range of moderate fields H_{dec} .

Fig. 7 Hysteretic dependences of **a** magnetoresistance $R(H)$ for the investigated sample at $T = 4.2$ K and **b, c** effective field $B_{\text{eff}}(H)$. In **b**, the $B_{\text{eff}}(H)$ dependences are built using Eq. (3) from the $M(H)$ data (Fig. 4b) at $\alpha = 25$ and 50. The $B_{\text{eff}}(H)$ dependence in **c** is built using the $\alpha(H)$ functional dependence from Fig. 8. Horizontal lines between symbols show determination of the field width ΔH of the hysteresis at $H_{\text{dec}} = 45$ and 20 kOe



Let us discuss a possible reason for the variation in the parameter α at $H = H_{dec}$. According to the critical state model [45, 54], at $H = H_{inc}$ (increasing external field), the external field penetrates in the form of Abrikosov vortices from the surface deep in the superconductor or, in our case, into each grain. As the field decreases ($H = H_{dec}$), the Abrikosov vortices remain mainly at the grain center. Possibly, in this case, their effect on the intergrain medium will manifest itself to a lesser extent, which will lead to a decrease in the parameter α . However, when the field direction changes from $H_{dec} \geq 0$ to $H_{inc} \leq 0$, the vortices start penetrating from the surface deep into the grains again [45, 54]. Therefore, we assumed that, starting with a certain field H_{1dec} , the parameter α (with decreasing H_{dec}) starts decreasing to a certain value α_{min} at $H_{dec} = 0$. Then, from $H = 0$ to field $|H_{1inc}|$, the parameter α grows to its maximum value α_{max} (the function continuity condition). According to our analysis, the $R(H)$ and $B_{eff}(H)$ hysteretic behaviors agree satisfactorily if we take $H_{1dec} \sim 20$ kOe, $H_{1inc} \sim 2$ kOe, $\alpha_{min} \sim 5$, and $\alpha_{max} \sim 50$ (these values can vary within $\sim 30\%$) in the above consideration. The $\alpha(H)$ functional dependence at the abovementioned H_{1dec} , H_{1inc} , α_{min} , and α_{max} values is shown in Fig. 8; the change in the parameter α from α_{min} to α_{max} was approximated by a linear function.

Figure 7c presents the $B_{eff}(H)$ dependence obtained by using the $\alpha(H)$ functional dependence shown in Fig. 8. Again, we observe good agreement both in the strong-field region (due to the value $\alpha_{max} = 50$) and in the moderate-field region (below 30–40 kOe). This is demonstrated by the comparison of the horizontal segment lengths at $H_{dec} = 20$ and 45 kOe in Fig. 7a, c. The aforesaid is illustrated in Fig. 9, which shows the $\Delta H(H_{dec})$ dependences obtained from the experimental $R(H)$ hysteretic dependence (Fig. 7a) and $B_{eff}(H)$ dependences at α values of 25 and 50, as well as from the $\alpha(H)$ functional dependence shown in Fig. 8.

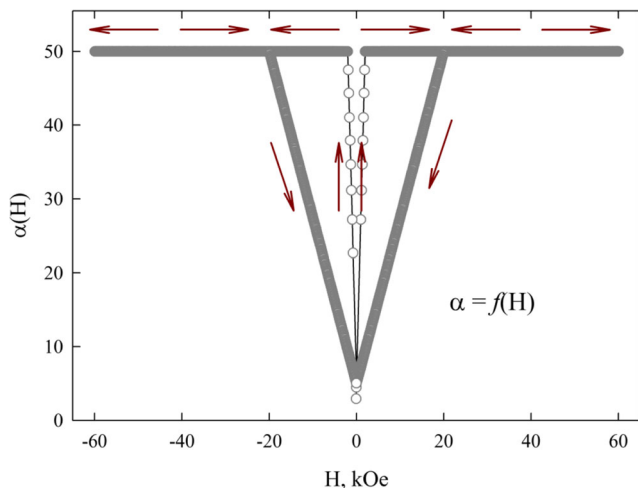


Fig. 8 The $\alpha(H)$ dependence used in building the $B_{eff}(H)$ dependence in Fig. 7c

Nevertheless, although the shape of the $R(H)$ dependence at $T = 4.2$ K (Fig. 7a) is similar to that in the high-temperature region (Fig. 5a), we should note the absence of a local maximum in the case of increasing field. The existence of this maximum is unambiguously caused by the $M(H_{inc})$ extremum, which is reflected on the $B_{eff}(H_{inc})$ behavior. The $B_{eff}(H_{inc})$ dependences shown in Fig. 7b, c contain a significant local maximum, which is not reproduced in the $R(H)$ curve at low temperatures.

In view of the aforesaid, it is interesting to follow the temperature evolution of the $R(H_{inc})$ local maximum. Figure 10 shows the $R(H)$ dependences obtained in the high-temperature region (scale R is on the left) and at $T = 4.2$ K (scale R is on the right); the abscissa axis is the logarithmic scale. The analysis of the high-temperature data allows us to conclude that, against the background of the increasing resistance with decreasing temperature, the local $R(H_{inc})$ maximum becomes more pronounced. Obviously, if the dissipation (the experimentally observed nonzero resistance) starts in the external field exceeding the maximum of the corresponding $B_{eff}(H_{inc})$ dependence, then this maximum will not be seen in the $R(H_{inc})$ dependence. According to Fig. 7c, we should expect the $R(H_{inc})$ maximum near $H_{inc} \sim 2$ kOe. For the helium temperature data in Fig. 9, the dissipation starts before the expected maximum. Possibly, the feature observed as a change in the $R(H_{inc})$ curvature sign (shown by an arrow in Fig. 10) reflects the $B_{eff}(H_{inc})$ maximum. The external field corresponding to this anomaly is ~ 4 kOe, which is stronger than the field of the $B_{eff}(H_{inc})$ maximum.

In addition, the absence of local $R(H_{inc})$ maximum can be explained as follows. Despite the sufficiently strong transport current in the magnetoresistance measurements at $T = 4.2$ K ($I = 175$ mA), the R value is no larger than 10% of the values obtained at 77 K ($I = 3$ mA; see Fig. 9). For comparison, the maximum resistive response R_{NGB} of the grain boundary

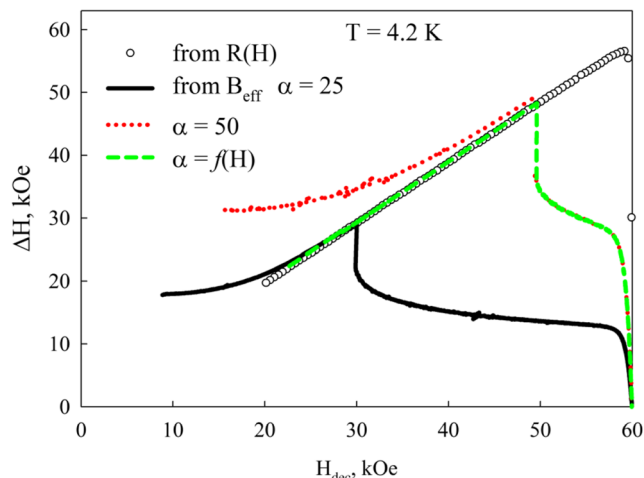


Fig. 9 Field dependence of the $\Delta H(H_{dec})$ hysteresis of the experimental $R(H)$ dependence at $T = 4.2$ K for the data from Fig. 7a (symbols) and effective field $B_{eff}(H)$ for the data in Fig. 7b, c

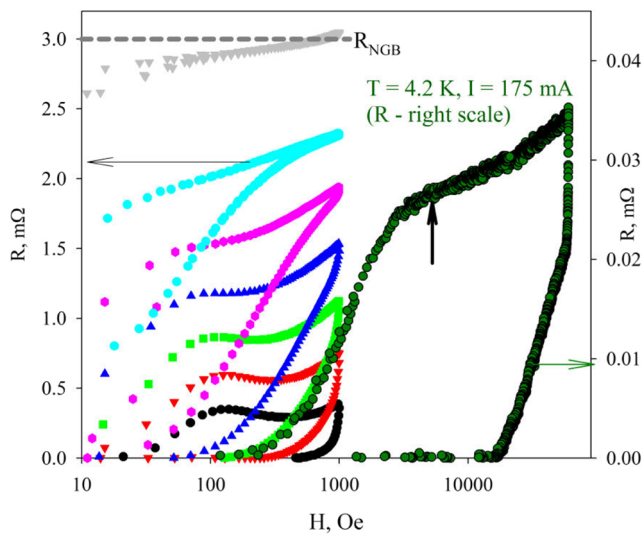


Fig. 10 $R(H)$ hysteretic dependences of the sample at different temperatures. The external field H is plotted on the abscissa axis in the logarithmic scale. The data for the maximum external field of $H_{\max} = 1000$ Oe were obtained at temperatures of 90, 88, 86, 84, 82, 80, and 77 K top-down (the transport current is $I = 3$ mA), and the R value for them is plotted on the left scale. The R_{NGB} value (see Fig. 2a) is also plotted on the left scale. For the data obtained at $T = 4.2$ K and $H_{\max} = 60$ kOe ($I = 175$ mA), the R value is plotted on the right scale. The vertical arrow shows the $R(H_{\text{inc}})$ feature discussed in the text

subsystem² is shown, which was obtained from the $R(T)$ data (the R_{NGB} value in Fig. 9 is plotted on the left scale). We may conclude from the data presented in Fig. 9 that the magnetoresistance observed at $T = 4.2$ K in an external field of 60 kOe is no higher than 1% of the R_{NGB} value. Possibly, at such a low sample resistance, the $B_{\text{eff}}(H_{\text{inc}})$ maximum cannot be seen because of redistribution of the microscopic transport current trajectories. This issue was considered in [55].

4 Conclusions

Thus, we examined the hysteretic behavior of magnetoresistance of the granular HTS of the classical yttrium system at different temperatures. In contrast to the previous works, this study was carried out also at a temperature of 4.2 K.

Our analysis of the $R(H)$ hysteresis using the developed model of the behavior of a granular HTS in an external magnetic field, in which the magnetoresistance is proportional to the effective field in the intergrain medium, showed the following. In the high-temperature region (77–90 K), the expression for the effective field $B_{\text{eff}}(H) = |H - 4\pi M(H) \alpha|$ (Eq. (3)) describes well the hysteretic behavior of magnetoresistance with regard to the experimental data on the $M(H)$ magnetic hysteresis. The numerical value of the parameter α (in this

² It is seen in Fig. 10 that at $T = 90$ K, the $R(H)$ dependence in fields of about 0.7 kOe crosses the line $R = R_{\text{NGB}}$. This is explained by the onset of dissipation in the HTS grains under these experimental conditions.

case, field-independent) in this expression is about 25. This is indicative of the considerable magnetic flux compression in the HTS intergrain medium. Interestingly, our result is consistent with the previous data [35] for a sample with the much better transport properties (the critical current density for the sample studied here is lower by an order of magnitude). Therefore, the magnetic flux compression in the intergrain spacing is a universal property typical of, at least, granular yttrium HTSs.

According to the analysis of the magnetoresistance hysteresis at low temperature (4.2 K), there are specific features inconsistent with the behavior predicted by the commonly accepted concept of the effective field, although the general form of the $R(H)$ hysteresis remains invariable. In particular, the expression for the effective field $B_{\text{eff}}(H)$ predicts a local maximum in increasing external field. At high temperatures, this agrees well with the observed magnetoresistance behavior, while at low temperature, this $R(H)$ feature is not observed. However, the maximum magnetoresistance at $T = 4.2$ K and $H = 60$ kOe is merely 1% of the full (maximum possible) resistance of the grain boundary subsystem. In addition, the obtained data showed that at low temperatures, it is necessary to take into account the dependence of the parameter α on the external field and there are strong grounds to believe that in the decreasing external field the α value becomes smaller. More thorough investigations of the $R(H)$ dependences at low temperatures and different transport current densities are needed to establish the true reason for this inconsistency.

The observed broad magnetoresistance hysteresis in the strong-field (up to 60 kOe) region showed that the degree of magnetic flux compression grows at low temperatures and the parameter α attains ~ 50 at $T = 4.2$ K. This result does not contradict the concepts of the dissipation processes in weakly bound superconducting systems, including the grain boundary subsystem with the effective grain boundary length decreasing with temperature [52, 53].

Funding Information The work was supported by the Russian Science Foundation (Grant No. 17-72-10050).

Publisher’s Note Springer Nature remains neutral with regard to jurisdictional claims in published maps and institutional affiliations.

References

1. Chaudhari, P., Mannhart, J., Dimos, D., Tsuei, C.C., Chi, J., Oprysko, M.M., Scheuermann, M.: Direct measurement of the superconducting properties of single grain boundaries in $\text{Y1Ba2Cu3O7-}\delta$. *Phys. Rev. Lett.* **60**(16), 1653 (1988)
2. De Vries, J.W.C., Stollman, G.M., Gijss, M.A.M.: Analysis of the critical current density in high-Tc superconducting films. *Physica C.* **157**, 406 (1989)

3. Petrov, M.I., Balaev, D.A., Krustalev, B.P., Aleksandrov, K.S.: The effect of heat treatment on the transport properties of the polycrystalline HTSC. *Physica C*. **235–240**, 3043 (1994)
4. Delin, K.A., Kleinsasser, A.W.: Stationary properties of high-critical-temperature proximity effect Josephson junctions. *Supercond. Sci. Technol.* **9**, 227 (1996)
5. Petrov, M.I., Balaev, D.A., Gokhfeld, D.M.: Andreev reflection and experimental temperature dependences of the critical current in heterogeneous high-temperature superconductors (polycrystals and related composites). *Phys. Solid State*. **49**, 619 (2007)
6. Dubson, M.A., Herbert, S.T., Calabrese, J.J., Harris, D.C., Patton, B.R., Garland, J.C.: Non-Ohmic dissipative regime in the superconducting transition of polycrystalline Y1Ba2Cu3Ox. *Phys. Rev. Lett.* **60**, 1061 (1988)
7. Jung, J., Mohamed, M.K., Cheng, S.C., Franck, J.P.: Flux motion, proximity effect, and critical current density in YBa2Cu3O7- δ /silver composites. *Phys. Rev. B*. **42**(N10), 6181 (1990)
8. Ji, L., Rzechowski, M.S., Anand, N., Tinkham, M.: Magnetic-field-dependent surface resistance and two-level critical-state model for granular superconductors. *Phys. Rev. B*. **47**, 470 (1993)
9. Sun, S., Zhao, Y., Pan, G., Yu, D., Zhang, H., Chen, Z., Qian, Y., Kuan, W., Zhang, Q.: The behaviour of negative magnetoresistance and hysteresis in YBa2Cu3O7- δ . *Europhys. Lett.* **6**(4), 359 (1988)
10. Qian, Y.J., Tang, Z.M., Chen, K.Y., Zhou, B., Qiu, J.W., Miao, B.C., Cai, Y.M.: Transport hysteresis of the oxide superconductor Y1Ba2Cu3O7-x in applied fields. *Phys. Rev. B*. **39**, 4701 (1989)
11. Celasco, M., Masoero, A., Mazzetti, P., Stepanescu, A.: Evidence of current-noise hysteresis in superconducting YBa2Cu3O7- δ specimens in a magnetic field. *Phys. Rev. B*. **44**, 5366 (1991)
12. Kuz'michev, N.D.: Critical state of Josephson medium. *JETP Lett.* **74**, 262 (2001)
13. Daghero, D., Mazzetti, P., Stepanescu, A., Tura, P., Masoero, A.: Electrical anisotropy in high-Tc granular superconductors in a magnetic field. *Phys. Rev. B*. **66**(13), 11478 (2002)
14. Derevyanko, V.V., Sukhareva, T.V., Finkel, V.A.: Magnetoresistance hysteresis of granular YBa2Cu3O7- δ high-temperature superconductor in weak magnetic fields. *Tech. Phys.* **53**, 321 (2008)
15. Shaikhutdinov, K.A., Balaev, D.A., Popkov, S.I., Petrov, M.I.: Mechanism of formation of a negative magnetoresistance region in granular high-temperature superconductors. *Phys. Solid State*. **51**, 1105 (2009)
16. Sukhareva, T.V., Finkel, V.A.: Hysteresis of the magnetoresistance of granular HTSC YBa2Cu3O7- δ in weak fields. *Phys. Solid State*. **50**, 1001 (2008)
17. Sukhareva, T.V., Finkel, V.A.: Phase transition in the vortex structure of granular YBa2Cu3O7- δ HTSCs in weak magnetic fields. *JETP*. **107**, 787 (2008)
18. Balaev, D.A., Popkov, S.I., Shaikhutdinov, K.A., Petrov, M.I., Gokhfeld, D.M.: Magnetoresistance of porous polycrystalline HTSC: effect of the transport current on magnetic flux compression in intergranular medium. *Phys. Solid State*. **56**, 1542 (2014)
19. Balaev, D.A., Semenov, S.V., Petrov, M.I.: Correlation between magnetoresistance and magnetization hysteresis in a granular high-Tc superconductor: impact of flux compression in the intergrain medium. *J. Supercond. Nov. Magn.* **27**, 1425 (2014)
20. Evetts, J.E., Glowacki, B.A.: Relation of critical current irreversibility to trapped flux and microstructure in polycrystalline YBa2Cu3O7. *Cryogenics*. **28**, 641 (1988)
21. Altshuler, E., Musa, J., Barroso, J., Papa, A.R.R., Venegas, V.: Generation of Jc (He) hysteresis curves for granular YBa2Cu3O7- δ superconductors. *Cryogenics*. **33**, 308–313 (1993)
22. Mune, P., Govea-Alcaide, E., Jardim, R.F.: Magnetic hysteresis of the critical current density of polycrystalline (Bi–Pb)–Sr–Ca–Cu–O superconductors: a fingerprint of the intragranular and intergranular flux trapping. *Physica C*. **354**, 275–278 (2001)
23. Mune, P., Fonseca, F.C., Muccillo, R., Jardim, R.F.: Magnetic hysteresis of the magnetoresistance and the critical current density in polycrystalline YBa2Cu3O7- δ -Ag superconductors. *Physica C*. **390**, 363–373 (2003)
24. Balaev, D.A., Gokhfeld, D.M., Popkov, S.I., Shaykhutdinov, K.A., Petrov, M.I.: Hysteretic behavior of the magnetoresistance and the critical current of bulk Y3/4Lu1/4Ba2Cu3O7+ CuO composites in a magnetic field. *Physica C*. **460–462**, 1307–1308 (2007)
25. Balaev, D.A., Dubrovskii, A.A., Popkov, S.I., Gokhfeld, D.M., Semenov, S.V., Shaykhutdinov, K.A., Petrov, M.I.: Specific features in the hysteretic behavior of the magnetoresistance of granular high-temperature superconductors. *Phys. Solid State*. **54**(11), 2155 (2012)
26. Balaev, D.A., Bykov, A.A., Semenov, S.V., Popkov, S.I., Dubrovskii, A.A., Shaikhutdinov, K.A., Petrov, M.I.: General regularities of magnetoresistive effects in the polycrystalline yttrium and bismuth high-temperature superconductor systems. *Phys. Solid State*. **53**(5), 922 (2011)
27. Lopez, D., De la Cruz, F.: Anisotropic energy dissipation in high-Tc ceramic superconductors: local-field effects. *Phys. Rev. B*. **43**(13), 11478 (1991)
28. Kiliç, A., Kiliç, K., Senoussi, S., Demir, K.: Influence of an external magnetic field on the current–voltage characteristics and transport critical current density. *Physica C*. **294**, 203–216 (1998)
29. Balaev, D.A., Prus, A.G., Shaykhutdinov, K.A., Gokhfeld, D.M., Petrov, M.I.: Study of dependence upon the magnetic field and transport current of the magnetoresistive effect in YBCO-based bulk composites. *Supercond. Sci. Technol.* **20**, 495 (2007)
30. Balaev, D.A., Popkov, S.I., Sabitova, E.I., Semenov, S.V., Shaykhutdinov, K.A., Shabanov, A.V., Petrov, M.I.: Compression of a magnetic flux in the intergrain medium of a YBa2Cu3O7 granular superconductor from magnetic and magnetoresistive measurements. *J. Appl. Phys.* **110**, 093918 (2011)
31. Balaev, D.A., Dubrovskii, A.A., Popkov, S.I., Shaikhutdinov, K.A., Petrov, M.I.: Relaxation of the remanent resistance of granular HTSC Y-Ba-Cu-O+ CuO composites after magnetic field treatment. *Phys. Solid State*. **50**, 1014–1021 (2008)
32. Balaev, D.A., Dubrovskii, A.A., Shaikhutdinov, K.A., Popkov, S.I., Gokhfeld, D.M., Gokhfeld, Y.S., Petrov, M.I.: Mechanism of the hysteretic behavior of the magnetoresistance of granular HTSCs: the universal nature of the width of the magnetoresistance hysteresis loop. *JETP*. **108**, 241 (2009)
33. Balaev, D.A., Semenov, S.V., Petrov, M.I.: Dominant influence of the compression effect of a magnetic flux in the intergranular medium of a granular high-temperature superconductor on dissipation processes in an external magnetic field. *Phys. Solid State*. **55**, 2422 (2013)
34. Balaev, D.A., Semenov, S.V., Pochekutov, M.A.: Anisotropy of the magnetoresistance hysteresis in the granular superconductor Y-Ba-Cu-O at different magnetic-field and transport-current orientations. *J. Appl. Phys.* **122**, 123902 (2017)
35. Semenov, S.V., Balaev, D.A.: Temperature behavior of the magnetoresistance hysteresis in a granular high-temperature superconductor: magnetic flux compression in the intergrain medium. *Physica C*. **550**, 19 (2018)
36. Mitin, A.V.: Effect of vortex dynamics on the transport properties of granular YBa2Cu3O7- δ with reduced Josephson junctions. *Physica C*. **235–240**, 3311 (1994)
37. Gaffney, C., Petersen, H., Bednar, R.: Phase-slip analysis of the non-Ohmic transition in granular YBa2Cu3O6.9. *Phys. Rev. B*. **48**, 3388 (1993)
38. Gamchi, H.S., Russell, G.J., Taylor, K.N.R.: Resistive transition for YBa2Cu3O7- δ -Y2BaCuO5 composites: influence of a magnetic field. *Phys. Rev. B*. **50**, 12950 (1994)
39. Balaev, D.A., Popkov, S.I., Semenov, S.V., Bykov, A.A., Sabitova, E.I., Dubrovskiy, A.A., Shaikhutdinov, K.A., Petrov, M.I.:

- Contributions from inter-grain boundaries to the magneto-resistive effect in polycrystalline high-T_c superconductors. The underlying reason of different behavior for YBCO and BSCCO systems. *J. Supercond. Nov. Magn.* **24**, 2129 (2011)
40. Prester, M., Babić, E., Stubičar, M., Nozar, P.: Dissipation in a weak-link-limited superconductor as a problem of percolation theory. *Phys. Rev. B.* **49**(N10), 6967 (1994)
 41. Derevyanko, V.V., Sukhareva, T.V., Finkel, V.A., Shakhov, Y.N.: Effect of temperature and magnetic field on the evolution of a vortex structure of the granular YBa₂Cu₃O_{7-δ} high-temperature superconductor. *Phys. Solid State.* **56**(N4), 649 (2014)
 42. Andrzejewski, B., Guilmeau, E., Simon, C.: Modelling of the magnetic behaviour of random granular superconductors by the single junction model. *Supercond. Sci. Technol.* **14**, 904–909 (2001)
 43. Dos Santos, C.A.M., Da Luz, M.S., Ferreira, B., Machado, A.J.S.: On the transport properties in granular or weakly coupled superconductors. *Physica C.* **391**, 345 (2003)
 44. Balaev, D.A., Popkov, S.I., Semenov, S.V., Bykov, A.A., Shaykhutdinov, K.A., Gokhfeld, D.M., Petrov, M.I.: Magnetoresistance hysteresis of bulk textured Bi_{1.8}Pb_{0.3}Sr_{1.9}Ca₂Cu₃O_x+Ag ceramics and its anisotropy. *Physica C.* **470**, 61–67 (2010)
 45. Bean, C.P.: Magnetization of high-field superconductors. *Rev. Mod. Phys.* **36**, 31 (1964)
 46. Senoussi, S.: Review of the critical current densities and magnetic irreversibilities in high T_c superconductors. *J. Phys. III France.* **2**, 1041 (1992)
 47. Chen, D.X., Cross, R.W., Sanchez, A.: Effects of critical current density, equilibrium magnetization and surface barrier on magnetization of high temperature superconductors. *Cryogenics.* **33**, 695 (1993)
 48. Gokhfeld, D.M.: An extended critical state model: asymmetric magnetization loops and field dependence of the critical current of superconductors. *Phys. Solid State.* **56**, 2380 (2014)
 49. Semenov, S.V., Balaev, D.A., Pochekutov, M.A., Velikanov, D.A.: Anisotropy of the magnetoresistive properties of granular high-temperature superconductors resulting from magnetic flux compression in the intergrain medium. *Phys. Solid State.* **59**, 1291 (2017)
 50. Balaev, D.A., Gokhfeld, D.M., Dubrovskii, A.A., Popkov, S.I., Shaikhutdinov, K.A., Petrov, M.I.: Magnetoresistance hysteresis in granular HTSCs as a manifestation of the magnetic flux trapped by superconducting grains in YBCO+CuO composites. *JETP.* **105**, 1174 (2007)
 51. Altinkok, A., Kiliç, K., Olutaş, M., Kiliç, A.: Magnetovoltage measurements and hysteresis effects in polycrystalline superconducting Y₁Ba₂Cu₃O_{7-x}/Ag in weak magnetic fields. *J. Supercond. Nov. Magn.* **26**, 3085 (2013)
 52. Barone, A., Paterno, J.: *Physics and Application of the Josephson Effect.* Wiley, New York (1982)
 53. Likharev, K.K.: Superconducting weak links. *Rev. Mod. Phys.* **51**, 101 (1979)
 54. Yeshurun, Y., Malozemoff, A.P., Shaulov, A.: Magnetic relaxation in high-temperature superconductors. *Rev. Mod. Phys.* **68**, 911 (1996)
 55. Semenov, S.V., Balaev, A.D., Balaev, D.A.: Dissipation in granular high-temperature superconductors: new approach to describing the magnetoresistance hysteresis and the resistive transition in external magnetic fields. *J. Appl. Phys.* **125**, 033903 (2019)